Medicinal Chemistry Research (2022) 31:1740–1753
https://doi.org/10.1007/s00044-022-02944-5

MEDICINAL CHEMISTRY RESEARCH

ORIGINAL RESEARCH

Bio-guided isolation of anti-Alzheimer's compounds from *Phyllanthus niruri* and role of niruriflavone in the reversal of aluminum chloride-induced neurobehavioral and biochemical changes in an animal model

Gayathri Rajamanickam[1] · Manju SL[1]

Received: 21 April 2022 / Accepted: 26 July 2022 / Published online: 24 August 2022

Abstract

Alzheimer's disease (AD) is one of the chronic neurodegenerative pathologies that lead to memory loss and mental and behavioral changes in elderly people. The senile plaques, neurofibrillary tangles, oxidative stress, increased acetylcholinesterase (AChE), and neuroinflammation by activating 5-lipoxygenases (5-LOX) are important pathological processes in AD. *Phyllanthus niruri* Linn (PN) earned a lot of attention for phytoconstituents and their medicinal properties. The compounds quercitrin and niruriflavone were isolated by bio-guided fractionation from PN using the in vitro assays. Both compounds showed good docking scores on AChE and 5-LOX targets in the molecular docking studies. AD was induced in rats by 100 mg/kg of oral aluminum chloride ($AlCl_3$) for 42 days. It decreased the antioxidative enzymes and increased lipid peroxidation and AChE activity. Oral administration of niruriflavone reversed the neurobehavioral changes caused by $AlCl_3$. The niruriflavone treatment also restored the antioxidative enzymes and attenuated the AChE and lipid peroxidation. All the evidence suggests that isolated compounds could benefit the population afflicted by AD in a multitargeted manner.

Graphical abstract

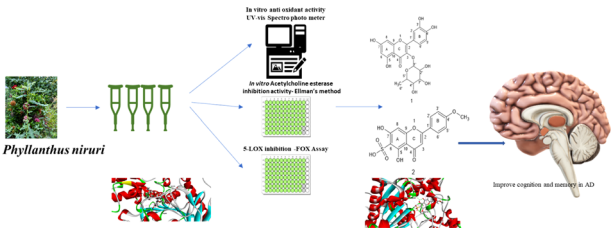

Keywords Alzheimer's disease · *Phyllanthus niruri* · Acetylcholinesterase · Lipoxygenase · Niruriflavone · Aluminum chloride

Introduction

Alzheimer's disease is one of the chronic neurodegenerative pathologies characterized by dementia and cognitive impairment, which primarily affects the elderly. It manifests with the formation of extracellular accumulation of β-amyloid (Aβ) plaque and intracellular accumulation of neurofibrillary tangles (NFT) via hyperphosphorylation of tau protein. In addition to the well-known pathology of senile plaques and NFT, oxidative stress is also a feature of AD brains [1]. Acetylcholinesterase (AChE) triggers the development of amyloid fibrils and the production of highly poisonous AChE-β amyloid complexes [2]. Chronic increases in AChE activity may aggravate hydrolysis of

✉ Manju SL
slmanju@vit.ac.in

[1] School of Advanced Sciences, VIT, Vellore, India

acetylcholine, a potential neurotransmitter in cerebral cortex cholinergic neurons, causing acetylcholine deficiency that leads to choline accumulation resulting in memory loss [3]. An excess of reactive oxygen species (ROS) causes neuroinflammation by activating lipoxygenases (LOXs), which influences the key mediators of inflammation [4]. Studies found the expression of LOX in the cerebral cortex and hippocampus of humans and rodents. 5-LOX expression rises with age. 5-LOX immunoreactivity is greater in both AD patients and AD mouse models, which is linked with the accumulation of Aβ plaques and NFTs. 5-LOX inhibition or deletion is linked to enhanced synaptic integrity markers and the recovery of AD-related memory impairments [5]. The data from the World Alzheimer's Report indicates that the prevalence of dementia will rise to 152.8 million by 2050, which was from 574 million in 2019 [6, 7]. The currently available AChE inhibitors, such as donepezil, galantamine, rivastigmine, and NMDA receptor antagonist memantine, have not been shown to be effective in disease-modifying processes rather than symptomatic relief. These drugs have major side effects such as sleeplessness, nausea, loss of appetite, diarrhea, muscle cramps, low blood pressure, breathing difficulties, and bradycardia. As a result, it's critical to develop preventive and therapeutic agents for AD. Herbal medicine is being studied all over the world, offering a wide variety of neuroprotective properties that might be beneficial for AD treatment and act by either directly activating antioxidant response genes or by enhancing the body's antioxidant defense system and anti-inflammatory action [8, 9]. Aluminum is a neurotoxicant and its exposure is thought to play a role in the etiology of Alzheimer's disease [10].

Phyllanthus niruri L. (PN), a member of the Euphorbiaceae family, has been used in the Ayurvedic system of medicine in India, as well as traditional Chinese and Indonesian medicine. It grows in the world's rain forests, in tropical and subtropical regions throughout the year [11]. The whole plant, fresh leaves, and fruits of this plant are used in folk medicine to cure various illnesses, including liver inflammation and other viral infections. It is said to contain an extensive series of phytoconstituents, including flavonoids such as quercetin, rutin, catechin, quercitrin, and astragalin; lignans such as phyllanthin and hypophyllanthin; and flavanone glycosides such as phyllanthenol. They have anti-inflammatory, antimicrobial, anticancer, antidiabetic, and lipid-lowering properties. They act as potent anti-oxidizing agents, as they have been found to be capable of scavenging superoxide anions and hydroxyl radicals, as well as chelating iron and boosting antioxidant enzymes in the human body [12–14]. Nevertheless, because of the complexity of AD pathology, single-targeted drugs can only provide palliative care rather than curative or preventive care.

After careful review of the literature, we sought to investigate the isolation of multitargeted antialzheimeric compounds from the whole plant of PN through bio-guided isolation and in vivo evaluation of nirurifiavone against Alzheimer's disease model.

Results and discussion

Bio-guided isolation using in vitro assays and characterization

The air-dried whole plant of PN was defatted using N-hexane followed by maceration with 70% alcohol and partitioned with organic solvents such as petroleum ether (PE), ethylacetate (EA), n-butanol (n-Bu), and water. The hydroalcoholic extract of the whole plant of PN was subjected to bio-guided fractionation and isolation (Fig. 1). The neuroprotective activity of four fractions was assessed by in vitro assays such as free radical scavenging activity using the 2,20-diphenyl-1-picrylhydrazyl (DPPH) assay, hydroxyl radical scavenging activity, AChE inhibition using Ellman's method, and 5-LOX inhibition using ferric oxidation of xylenol orange (FOX). The IC_{50} values of the EA fraction in all four assays were comparatively less than the other three fractions (Table 1). EA fraction showed greater inhibition activity on all four assays. So, EA fraction was further fractionated into five fractions by column chromatography using Sephadex LH (SLH-20), and the eluent used was chloroform: methanol (1:1). From the thin layer chromatography (TLC) analysis, fractions were pooled according to their separation profile. In vitro inhibitory assays were performed on fractions 1–5 and 1–6. Among all, fractions 2 and 5 were found to be more active. Based on the TLC, fraction 2 was further recrystallized with water to provide isolated compound 1. Fraction 5 was further subjected to SLH-20 column chromatography using methanol and water (1:1) to gain fractions 5.1–5.3 and analyzed for activities. Fractions 5.1 showed potent activity. The purification of fraction 5.1 by open column chromatography with dichloromethane and methanol to get the isolated compound 2. The two isolated compounds were evaluated for neuroprotection using all four mentioned assays. The IC_{50} of compound 1 for DPPH and hydroxyl-free radical for antioxidant activity, AChE inhibition, and 5-LOX inhibitions were found to be 18.34 ± 0.74, 25.03 ± 1.8, 34.8 ± 1.26, and 41.88 ± 1.24, respectively, whereas the IC_{50} values of compound 2 were 14.46 ± 0.29, 19.37 ± 1.32, 17.67 ± 6.2, and 37.55 ± 0.88, respectively. They are comparable with the IC_{50} values of positive controls and were shown in Table 1. The IC_{50} values of compound 2 is lower than compound 1. So, compound 2 can have better neuroprotective activity in comparison with compound 1.

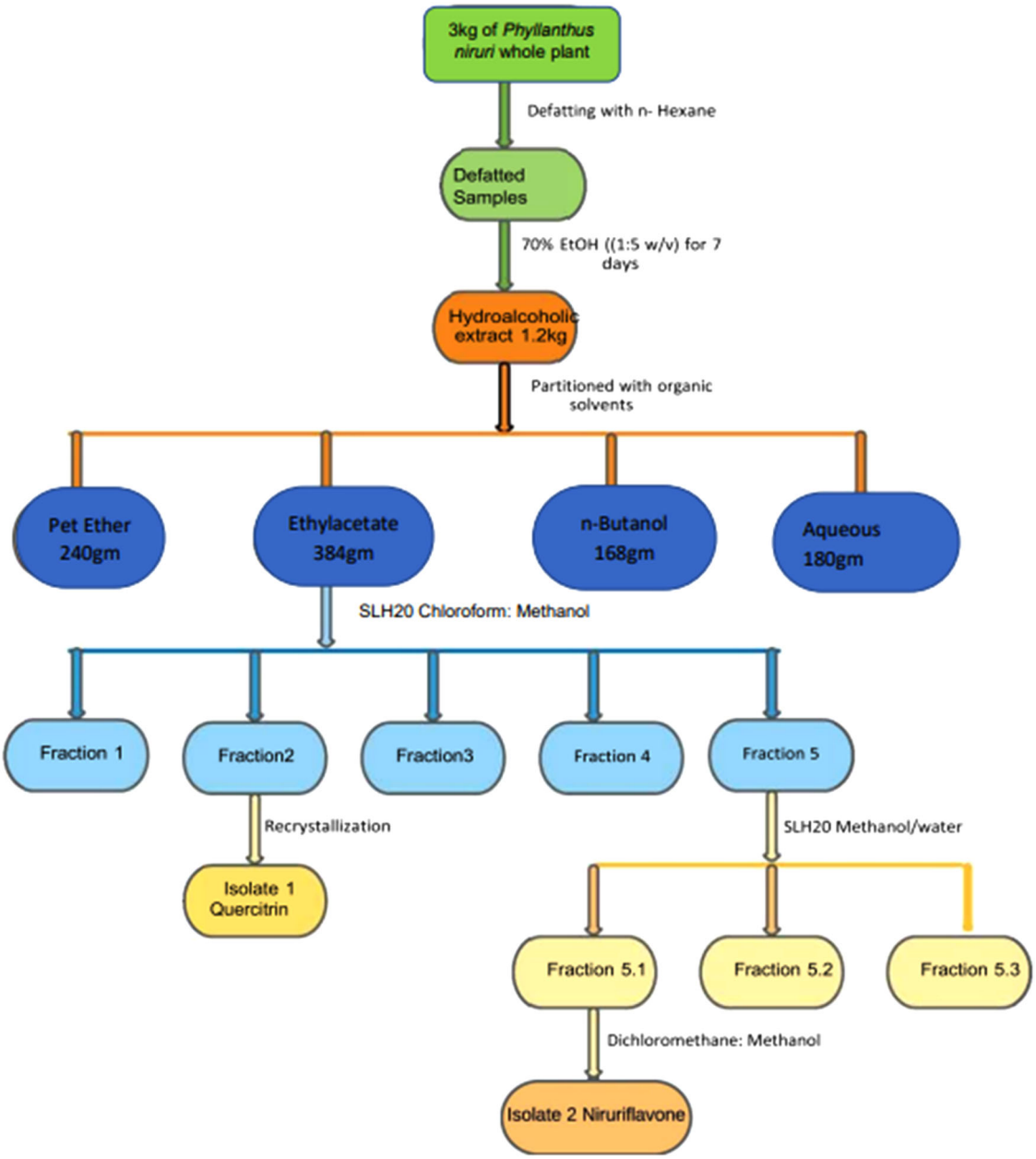

Fig. 1 Flowchart for isolation of anti-Alzheimer's compounds from *Phyllanthus niruri* Linn

The structures of purified compounds were confirmed by infrared (IR) spectroscopic techniques, nuclear magnetic resonance (NMR), and high-resolution electron ionization mass spectra (HREI-MS) by comparing with the existing literature [15–17]. The isolated compound 1 was identified as quercitrin and compound 2 was niruriflavone (Fig. 2).

The isolated compound 1 appeared yellow in color and in powder form. The yield of the isolated compound was found to be 1.51 g. The molecular formula, $C_{21}H_{20}O_{11}$, of compound 1 was obtained from HREI-MS, which exhibited a $[M]^+$ peak at m/z 448, calculated at 448.36 g/mol. In IR spectra, the existence of hydroxyl (OH) at 3410 cm^{-1} and carbonyl (C=O) group at 1643 cm^{-1} were detected. The peak at 2925 cm^{-1} denoted the stretching of C-H, 1448 cm^{-1} for the C=C ring, 1105 cm^{-1} for C-O-C stretching, and 812 cm^{-1} for substituted benzene. ^1H NMR spectral data of compound 1 displayed the five aromatic peaks at δ 7.30 (H-2′), 7.26 (H-6′), 6.9 (H-5′), 6.4 (H-8), and 6.21 (H-6) and the presence of a peak at 5.26 (H-1″), 4.6 (H-2″), 3.5 (H-3″), 3.24 (H-5″), 3.18 (H-4″), and 0.89 (Me-6″) along with ^{13}C NMR signals at 101.1 (C-1″), 69.6 (C-2″), 72.2 (C-3″,C-4″), 73.8 (C-5″), and 18.1 (C-6″,CH_3) confirmed the existence of rhamnose moiety in quercitrin.

Table 1 IC_{50} of in vitro antioxidant, acetylcholinesterase, and 5-lipoxygenase inhibition activities

Extracts/ isolate/standard	DPPH radical scavenging activity (µg/ml)	Hydroxyl radical scavenging activity (µg/ml)	Acetylcholinesterase inhibition activity (µg/ml)	5-Lipoxygenase inhibition activity (µg/ml)
Pet ether	295 ± 5.7	97.09 ± 0.86	370.73 ± 2.41	662.7 ± 1.8
Ethylacetate	68 ± 2.8	60.5 ± 1.25	158.87 ± 1.37	270.4 ± 2.3
n-butanol	243 ± 5.2	75.20 ± 0.17	201.35 ± 1.8	400.1 ± 4.2
aqueous	270 ± 1.9	94.7 ± 1.28	230.25 ± 2.32	460.9 ± 5.8
F 1	335.42 ± 4.25	100.6 ± 0.43	482.12 ± 9.12	201.8 ± 1.8
F 2	25 ± 12.3	43.8 ± 1.15	37.23 ± 3.40	58.62 ± 0.15
F 3	213 ± 11.4	74.40 ± 0.23	265.12 ± 2.39	63.25 ± 9.11
F 4	143 ± 1.2	69.84 ± 1.30	280.74 ± 1.16	94.8 ± 0.4
F 5	135 ± 12.3	48.2 ± 1.45	55.44 ± 0.17	109.4 ± 1.4
F 5.1	15.2 ± 3.5	28.2 ± 1.3	105.03 ± 1.20	43.99 ± 0.79
F 5.2	54.5 ± 7.2	59.84 ± 2.03	160.19 ± 1.81	90.25 ± 0.11
F 5.3	31.01 ± 0.90	39.40 ± 1.51	118.61 ± 2.01	45.46 ± 0.75
Isolate 1	18.34 ± 0.74	25.37 ± 1.8	34.38 ± 1.26	41.88 ± 1.24
Isolate 2	14.46 ± 0.29	19.3 ± 1.32	17.67 ± 6.2	37.55 ± 0.88
Std ascorbic acid	12.68 + 0.01	16.25 ± 1.01	–	–
Positive control	–	–	16.50 ± 0.25	–
	–	–	–	69.7 ± 0.3

Each value is expressed as mean ± SEM ($n = 3$). The IC_{50} value was determined from linear regression analysis using Microsoft Excel

Fig. 2 Structures of isolated compounds

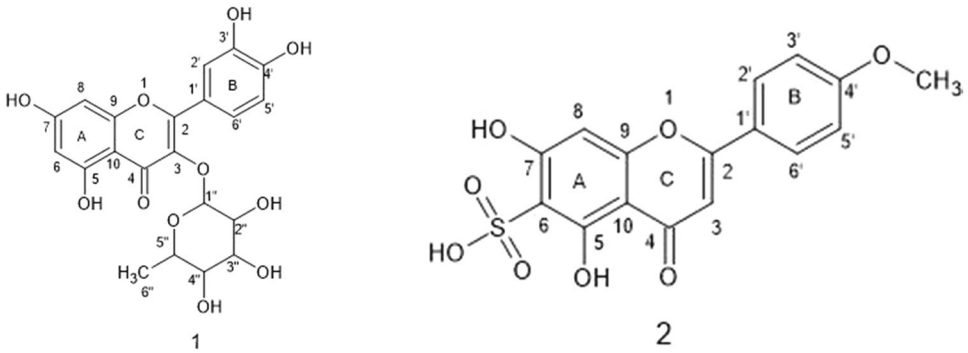

The isolated compound 2 was a yellowish powder. The yield of the compound was 1.18 g. The molecular formula $C_{16}H_{12}O_8$ S of compound 2 was obtained from HREI-MS, which indicated a $[M]^+$ peak at m/z 364 calculated 364.32 g/mol. In IR spectra, the presence of sulphonyl (S=O) and carbonyl (C=O) groups was detected at 1372 and 1634 cm^{-1}, respectively. The peak at 3542 cm^{-1} (OH str), 1077 cm^{-1} (S-O str), 3315 cm^{-1} (Ar C-H str), and 846 cm^{-1} (Ar C-H bend) were observed in the spectra. ^1H NMR spectrum of compound 2 showed two singlets at 12.93 and 10.86 that were related to the 5-OH and 7-OH. The doublet peak at 8.03 and 7.11 represented the aromatic proton at 2′,6′ and 3′,5′. The presence of methoxy group at 4′ was confirmed by the singlet peak at 3.86. The ^{13}C NMR spectrum displayed sixteen signals including the peak at 114.36 that represented the sulfonate group in C-6. The presence of C=O at fourth position, C at 4′ and OCH_3 at 4′ were confirmed by the peaks at 181.95, 159.87, and 56.22, respectively.

Abnormal free radical formation causes significant tissue and biomolecule damage in biological systems, leading to degenerative diseases [18]. Studies found that Aβ (1–42), microglial activation, iron overload, and mitochondrial dysfunction are linked to increased oxidative stress by oxidant production in AD [19]. In vivo studies, the hydroxyl-free radical can initiate lipid peroxidation (LPO), which causes significant cell damage. DPPH is a frequently used model system for determining the ability of phyto-constituents to scavenge free radicals [18]. In our research, we determined the antioxidant activity of quercitrin and

niruriflavone by DPPH and hydroxyl radical assays using spectrophotometry in three different concentrations: 125, 250, and 500 µg/ml. The standard drug taken for studies was ascorbic acid. The compounds inhibited the free radicals. If the concentration of the compounds was increased, the percentage inhibition of the compounds was also increased. The compounds with a lesser IC_{50} value had better inhibition activities. The identified compounds exert an antioxidant property by scavenging a significant amount of DPPH by electron transfer or hydrogen donation. The isolated compounds act by quenching the hydroxyl radicals that prevent LPO [20, 21]. The existence of catechol hydroxyl groups at positions C-3′ and 4′ in the B ring, double bond at 2 and 3 in ring C, and the number and position of hydroxyl groups at rings A and B are responsible for the significant antioxidant activity of the two isolated compounds. The methoxy group at 4′ in niruriflavone expels the effect of a metabolizing enzyme that might be responsible for the enhanced antioxidant capacity of that compound. We found that the antioxidant activity of quercitrin is less than that of niruriflavone. It indicates that antioxidant capacity is greatly ascertained by the number of phenolic hydroxyls [22]. Earlier studies by Noreen et al. showed that the substitution of methoxy group in phenolic hydroxyls of ring B had a greater impact on antioxidant activity [23].

5-LOX is responsible for Alzheimer's disease-related neuroinflammation. Earlier investigations have proven the reduction of astrocytosis and microgliosis in AD-induced rat brains by altering the LOX pathway. 5-LOX inhibitors appear to have the greatest anti-inflammatory potential in human fetal microglia. This indicates the importance of these enzymes in regulating proinflammatory responses in inflammatory conditions like neurodegenerative diseases [24]. The inhibition activity of 5-LOX by isolated compounds at different concentrations, from 125 to 500 µg/ml depends on compound concentration. The catechol hydroxyl groups and planarity to the molecules by carbon double bonds (C=C) at positions 2 and 3 can be the structural traits that provide the flavonoids' LOX inhibitory activity [25]. The activity of quercitrin was considerably reduced in comparison with niruriflavone.

Acetylcholine deficiency has a significant influence on short-term memory and learning. Some symptoms of AD might be alleviated by impeding the enzyme for the breakdown of acetylcholine [26]. The mechanism behind the beneficial role of flavonoids can be conferred by the catechol group on the B ring and the OH group at the seventh position of the isolated flavonoid compounds [27]. The presence of a sulfonic acid group is essential to enhancing enzyme actions [28]. Sulfate phenolic compounds act as cellular metabolism modulators, which play a role in preventing AD progression [29]. The sulfonic group found in niruriflavone is also one of the primary reasons for its potent neuroprotective activity.

Niruriflavone and quercitrin from PN can be multi-target-directed ligands that are capable of concurrently dealing with various vital AD pathologies as depicted previously, with improved efficacy or safety compared to drugs that focus on only a single target. Niruriflavone with lower inhibition activities in oxidative stress, AChE, and 5-LOX is more potent than Quercitrin. So niruriflavone has been evaluated for further studies.

Molecular docking

Using Discovery Studio suite 4.5 software, a molecular docking study was conducted to better understand the binding mode of isolated compounds within the active site of AChE and 5-LOX. Protein Data Bank (PDB) was used to obtain the X-ray crystal structure of AChE complexed with galantamine (PDB code: 1QTI) and S663D Stable-5-LOX in complex with Arachidonic Acid (PDB code: 3V99). The CHARMm forcefield was used to calculate the -CDOCKER score, which was then used to rank the poses of each input ligand. The -CDOCKER energy is based on the internal ligand strain energy and receptor-ligand interaction energy. The energy of the nonbonded interaction between the protein and the ligand is also denoted by the -CDOCKER interaction. A higher -CDOCKER energy and -CDOCKER interaction energy value indicates a more favorable protein-ligand interaction [30, 31]. The -CDOCKER energy and -CDOCKER interaction energy energies of quercitrin and niruriflavone showed that the best docking scores on both enzyme targets would be the best candidates for biological activity testing (Table 2). According

Table 2 Molecular docking studies of quercitrin and niruriflavone with AChE

Compound	AChE		5-LOX	
	-CDOCKER energy (kcal/mol)	-CDOCKER interaction energy (kcal/mol)	-CDOCKER energy (kcal/mol)	-CDOCKER interaction energy (kcal/mol)
Quercitrin	19.478	61.8307	5.95806	52.1786
Niruriflavone	28.7985	42.1382	31.25	42.3827
Cocrystal ligand	–	46.5862	–	55.0741
Positive controls	30.7497	39.6666	26.2481	26.5795

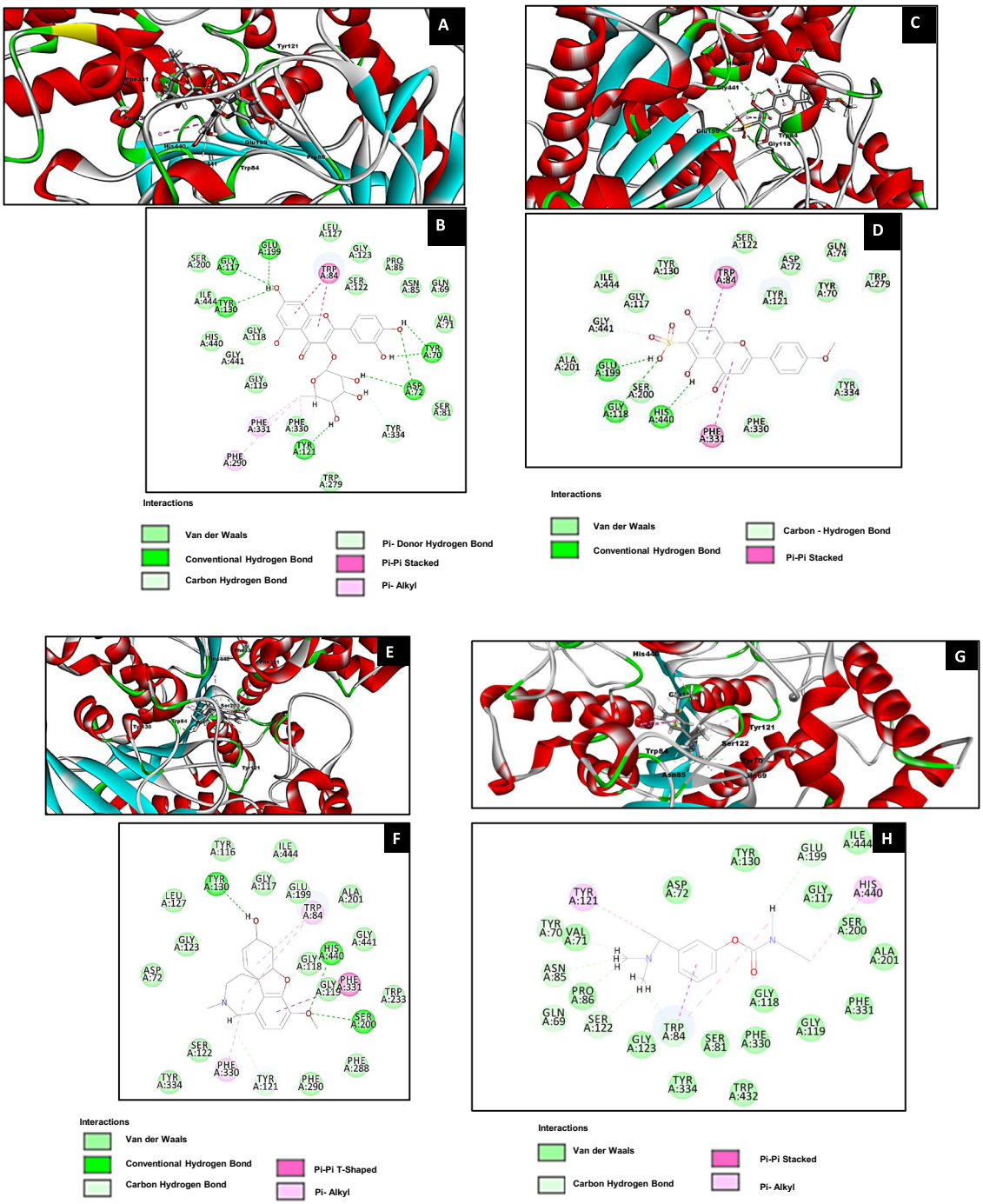

Fig. 3 3D and 2D representations of quercitrin (**A**, **B**); niruriflavone (**C**, **D**); cocrystal ligand (**E**, **F**); positive control (**G**, **H**) docked with AChE

to the findings, Niruriflavone had the highest -CDOCKER energy to the AChE and 5-LOX. The hydrogen bond interaction of the protein-ligand complex was also evaluated, followed by a binding mode analysis. The interactions of AChE with ligand reveal that the residues Glu199, Gly118, and His 440 were involved in the formation of hydrogen bonds with the niruriflavone whereas the residues Glu199, Gly117, Tyr 130,70,121, and Asp72, respectively, involved in the formation of hydrogen bonds with the quercitrin (Fig. 3). The interactions of 5-LOX with ligand were shown (Fig. 4). The compounds showed a promising favorable interaction with the AChE binding site and 5-LOX binding site. Binding the active sites of AChE and 5-LOX enzymes niruriflavone inhibits AChE and 5-LOX. This finding is in line with in vitro inhibitory activity. These results revealed that compounds were potential molecules to treat AD.

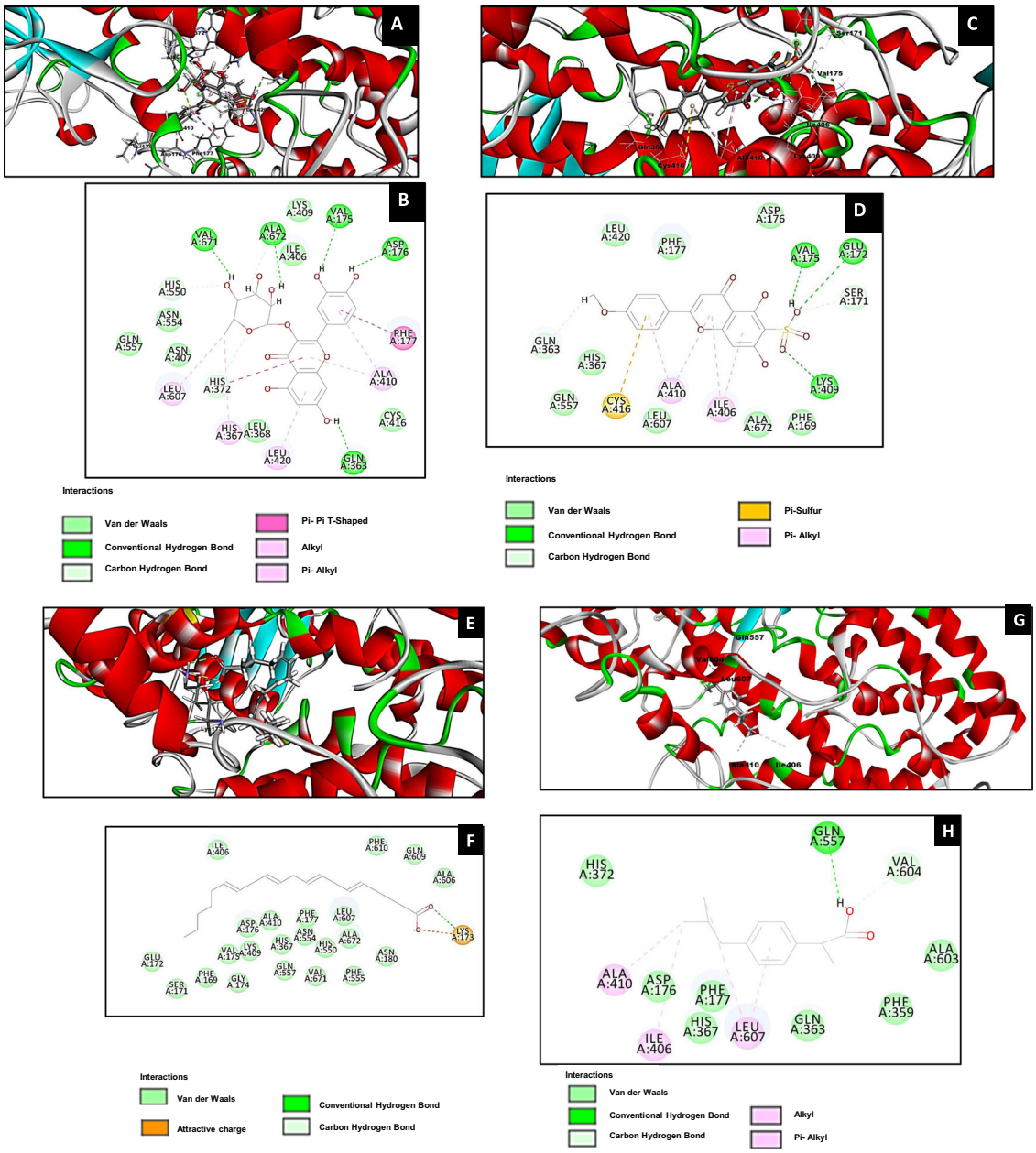

Fig. 4 3D and 2D representations of quercitrin (**A**, **B**); niruriflavone (**C**, **D**); cocrystal ligand (**E**, **F**); positive control (**G**, **H**) docked with 5-LOX

In vivo studies

Effect of niruriflavone on neurobehavioral studies

Based on in vitro and docking experiments, niruriflavone outperformed quercitrin in terms of neuroprotective efficacy. As a result, niruriflavone was employed in additional in vivo experiments in the Wister rat with aluminum chloride ($AlCl_3$) caused AD. Prolonged oral administration of $AlCl_3$ causes learning and memory skills to deteriorate, as evidenced by the literature reports cited in this study. In the Morris water maze (MWM) task, $AlCl_3$-treated rats ($p < 0.001$) had a significantly longer time to reach the platform and lesser time spent in the target quadrant that indicating learning and memory deficits than the normal control group rats. However, niruriflavone ($p < 0.01$) at the dose of 0.125 mg/kg/bodyweight provided significant protection from $AlCl_3$-induced learning and memory deficits in treated groups. The entry to open arm ($p < 0.01$) and closed arms ($p < 0.01$) by $AlCl_3$ treated rats were lesser and greater, respectively, than in the control groups. The time spent ($p < 0.001$) in the open arm by $AlCl_3$-induced rats was less and in the closed arms ($p < 0.001$) was more in comparison to the control group. The treatment with niruriflavone

Table 3 Effect of niruriflavone on neurobehavioral studies

Groups	Morris water maze test		Elevated plus maze test			
	Time taken to reach platform (s)	Time spent in the target quadrant (s)	Number of entries		Time spent (s)	
			Open arm	Closed arm	Open arm	Closed arm
Group I	16.87 ± 0.757	27.40 ± 0.945	6.167 ± 0.601	4.833 ± 0.671	84.167 ± 2.205	90 ± 2.288
Group II	41.067 ± 2.034[a]	13.833 ± 1.093[a]	3.50 ± 0.288[b]	7.167 ± 0.289[b]	35 ± 2.887[a]	130.933 ± 2.13[a]
Group III	29.046 ± 2.130[d]	17.20 ± 0.987[d]	5.167 ± 0.441	5.90 ± 0.208	79.90 ± 1.242[c]	92.833 ± 1.481[c]
Group IV	27.10 ± 1.646[c]	22.067 ± 1.593[d]	5.70 ± 0.351[e]	5.067 ± 0.636[e]	81.267 ± 2.034[c]	90.667 ± 2.33[c]

Data are expressed as mean ± SEM $n = 6$, one-way ANOVA followed by Dunnett's test

[a]$p < 0.001$, [b]$p < 0.01$ as compared with normal control; [c]$p < 0.001$,[d]$p < 0.01$, [e]$p < 0.05$ as compared with disease control

($p < 0.001$) in the $AlCl_3$-induced rats showed protective effects. These results were available for the positive control rivastigmine-treated rats (Table 3).

Using behavioral tests, including the MWM, and elevated plus maze (EPM) we investigated the behavioral changes caused by chronic aluminum exposure and the possible effect of niruriflavone treatment. Aluminum is a cholinotoxin and it is one of the environmental factors that is linked to neurodegenerative diseases like AD. Chronic administration of aluminum increases oxidative stress in the brain and causes neuronal inflammation. It impairs working memory, attention, and semantic memory. It also causes changes in cholinergic and noradrenergic neurotransmission and alters the blood–brain barrier's function [32–34]. It causes severe neurotoxicity by impairing glucose utilization, increasing free radical generation and LPO, as well as changes in phosphoinositide metabolism and protein phosphorylation. It was confirmed in this present study, aluminum exposure by oral administration of aluminum chloride to the rats was linked to decreased spatial memory and working memory in MWM. Furthermore, the exposure to aluminum triggered the anxiety-related symptom in AD rats that were observed in EPM. We discovered that niruriflavone-treated rats protected their spatial learning abilities and recovery of anxiety. These findings support the neuroprotective role of niruriflavone in the treatment of cognitive impairments in AD.

Effect of niruriflavone on acetylcholinesterase (AChE) activity

Chronic $AlCl_3$ treatment significantly increased AChE activity than the control group implying that $AlCl_3$ caused significant memory impairment. However, niruriflavone ($p < 0.01$) treatment significantly diminished AChE activity when compared to $AlCl_3$-induced AD rats (Fig. 5). The administration of the currently available drug rivastigmine ($p < 0.001$) also attenuated the activity of AChE in the brain. Learning, memory, and cognition are all influenced by cholinergic transmission. The severity of dementia in patients is related to the degree of impairment in this cholinergic transmission. The powerful cholinotoxin aluminum cause changes in cholinergic and noradrenergic transmission by altering the blood–brain barrier. So, it significantly increases AChE activity, the key enzyme involved in acetylcholine hydrolysis. It could be due to interactions between aluminum and AChE peripheral sites that change AChE's secondary structure, increasing its activity. Astoundingly, the oral administration of niruriflavone to $AlCl_3$-induced AD rats resulted in a significant decline in AChE [35–37].

Effect of niruriflavone on the biochemical markers of oxidative stress in Alzheimeric rats

The levels of the oxidative stress marker malondialdehyde (MDA), as well as the oxidative stress enzymes such as Catalase (CAT), and Superoxide dismutase (SOD were measured in the brain tissues of animals. In a comparison to control rats, the intoxicated rats had a significant increase in MDA levels and a suppression in SOD and CAT levels (Fig. 5). The oral administration of niruriflavone to AD animals resulted in a significant reduction in MDA levels and an improvement in SOD and CAT levels in the brain tissues.

The pathology of many neurodegenerative disorders including AD is linked to the accumulation of ROS and macromolecular oxidative damage. GSH and CAT are the most common endogenous antioxidants. MDA is produced by LPO in response to ROS that cause injury and membrane degradation. Aluminum accelerates the LPO and causes an increase in free radical accumulation, resulting in oxidative stress and neurotoxicity. The brain is extremely vulnerable to oxidative stress, which is caused by an increase in free radical levels and a decrease in antioxidant levels, resulting in toxicity [34, 38]. So, the compounds that are to combat ROS might be good candidates to treat AD. Niruriflavone mitigated the oxidative product MDA and increased the level of antioxidant enzymes such as SOD and CAT.

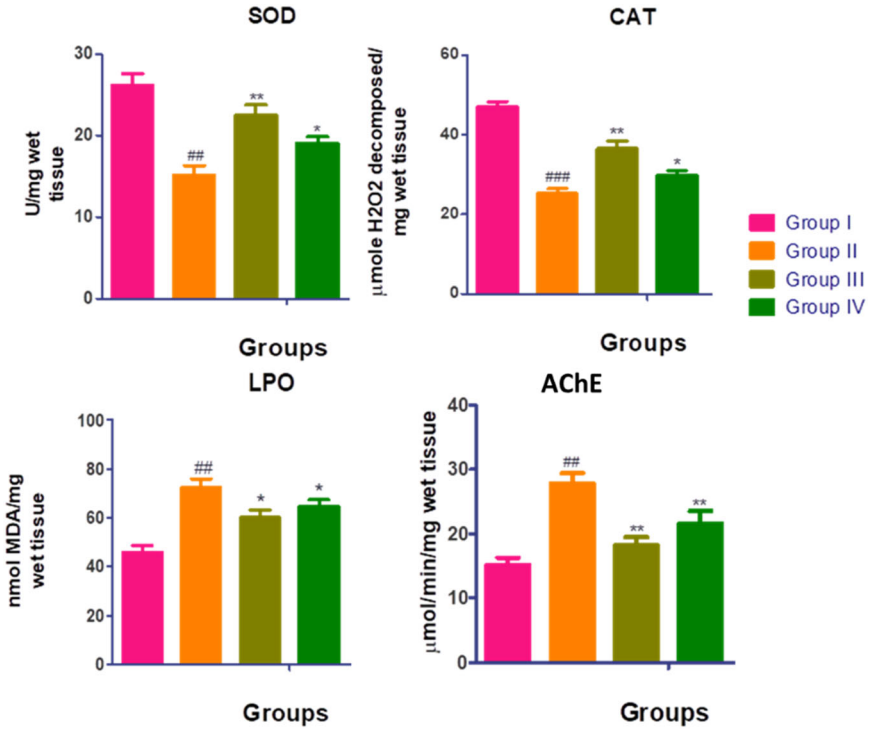

Fig. 5 Effect of niruriflavone on the biochemical markers of oxidative stress in Alzheimeric rats. $^{###}p < 0.001$, $^{##}p < 0.01$ as compared to control; $^{**}p < 0.01$ as compared to disease control

Conclusion

A bioassay-guided approach was used to identify the neuroprotective components of *P. niruri* in this investigation. This is the first study to assess the neuroprotective activity of quercitrin and niruriflavone in PN through a multi-targeted approach. The isolated compounds show oxidative damage reduction, and inhibition of AChE and 5-LOX. The above-said actions play a vital role in the prevention and treatment of AD. Both quercitrin and niruriflavone showed good inhibition activities. Quercitrin and niruriflavone can be potent neuroprotective agents. Niruriflavone responds better than quercitrin to oxidative stimuli, AChE enzyme, and inflammatory situations. Molecular docking studies also proved the binding affinity of isolated compounds from PN with the active sites of AChE and 5-LOX. In vivo application of niruriflavone on $AlCl_3$ induced AD rats to reduce AChE and oxidative stress, all of which are important in the progression of Alzheimer's disease. This study opens the door to the possibility of using niruriflavone to mitigate the complex pathological mechanism of a neurodegenerative disorder like AD. However, further studies are needed to validate the effect of long-term inhibition of AChE and 5-LOX. Using plant-derived flavonoids in multitargeted drug approaches for Alzheimer's disease treatment could be a novel study and steppingstone in the field of neurodegenerative disorders. The discovery of potent multitargeted neuroprotective agents could benefit the population afflicted by AD.

Materials and methods

General experimental procedures

All the solvents and chemicals used in the study were of analytical grade. For TLC, we used the Merck pre-coated silica gel 60 F254 plates. On silica gel 60 (70–230 mesh) and Sephadex LH-20 column chromatography were performed. Ascorbic acid, donepezil, rivastigmine, and ibuprofen were used as positive control. Veeco VMP-1 Apparatus was used to determine the melting points of the isolated. The melting points are expressed in °C and were uncorrected. The IR spectra of compounds were obtained using the KBr pellet technique and were represented in cm^{-1} using a Shimadzu FT-IR spectrophotometer. ^{1}H, ^{13}C, and NMR spectra were obtained in Bruker at 400 and100 MHz respectively using DMSO.UV spectroscopy was performed on a Shimadzu spectrophotometer. A BioRad microplate reader was used for in vitro assays. The molecular weight was determined by HREI-MS.

Plant material

The whole plant of *P. niruri* Linn (Euphorbiaceae) was gathered from farm fields around Erode district of Tamilnadu state in India between October to December and authenticated by pharmacognosy division of SKM Siddha and Ayurveda company (India) private limited, Erode. The collected fresh whole plants of *P. niruri* were washed with

distilled water and then dried in shade for 7–10 days then ground to powder.

Extraction, fractionation, and isolation of *Phyllanthus niruri* Linn

The powdered whole plant of *P. niruri* was defatted with N-Hexane. They were macerated with 70% EtOH (1:5 w/v) at room temperature for 7 days with intermittent shaking to obtain a hydroalcoholic extract of PN (HAPN). The HAPN evaporated under reduced pressure to yield a residue. The residue was mixed with water (50 ml) and partitioned successively with organic solvents such as PE, EA, and n-Bu (a total of two aliquots of 100 ml each) using a separating funnel. At the end of the fractionation process, we obtained the yield of four fractions as follows: PE (240 g), EA (384 g), n-BuOH (168 g), and water (180 g). Among these four fractions, the EA fractions were found to be the most potent in the four in vitro assays. The EA fraction was further separated with an SLH-20 column, using a mixture of chloroform and methanol (1:1) to give various fractions. From the TLC analysis, fractions were combined according to their separation profile and performed on all four assays to identify the potent fractions. Based on the assay, fractions 2 and 5 were identified as potent fractions. Purification of fraction 2 yielded compound 1. Fraction 5 was separated on an SLH-20 gel by column chromatography with methanol and water (1:1) to obtain fractions 5.1–5.3. Among the three fractions, fraction 5.1 showed strong inhibition activity in assays. Further purification of fraction 5.1 using open column chromatography with dichloromethane and methanol yielded compound 2.3.4.

Physical and spectroscopic data of compounds 1 and 2

Quercitrin (1): yellow powder; m.p 180–185 °C; IR (KBr) 3410,1643, 2925, 812, 1105, 1448,1383, 1217 cm^{-1}; ^{1}H NMR (400 MHz, DMSO) δ 12.65 (1H, s, 5-OH), 6.21 (1H, d, J = 2 Hz, H-6), 10.85 (1H, s, 7-OH), 6.4 (1H, d, J = 2 Hz, H-8), 7.30 (1H, d, J = 2 Hz, H-2′), 7.26 (1H, dd, J = 8.4, 2.4 Hz, H-6′), 6.9 (1H, d, J = 8 Hz, H-5′), 5.26 (1H, d, J = 0.8 Hz, H-1″), 4.6 (1H, d, J = 5.6, Hz, H-2″), 3.5 (1H,t, J = 4 Hz, H-3″), 3.24 (1H,dd, J = 6 Hz,12, H-5″), 3.18 (1H, dd, J = 5.6, 12 Hz, H-4″), 0.89 (3H, d, J = 8.0 Hz, Me-6″); ^{13}C NMR (100 MHz, DMSO) δ 158.5 (C, C-2), 136.2 (C, C-3), 179.6 (C, C-4), 163.2 (C, C-5), 99.8 (C, C-6), 165.8 (C, C-7), 94.7 (C, C-8), 159.3 (C, C-9), 105.9 (C, C-10), 122.9 (C, C-1′), 117.0 (C, C-2′), 146.4 (C, C-3′), 149.8 (C, C-4′), 123.0 (C, C-5′), 116.4 (C, C-6′), 103.5 (C, C-1″), 71.9 (C, C-2″), 72.1 (C, C-3″), 73.3 (C, C-4″), 72 (C, C-5″), 18.1 (C, C-6″ CH_3); HREI-MS found m/z 448 calculated for $[M]^+$ $C_{21}H_{20}O_{11}$ calculated molecular weight: 448.36 g/mol.

Niruriflavone (2): yellow powder; m.p 293–296 °C; IR (KBr) 1634.07, 3542.61, 3315, 846.15, 2237.15, 1372, 1077.53, 1110.84 cm^{-1}; ^{1}H NMR (400 MHz, DMSO) δ 12.93 (1H, s, 5-OH), 10.86 (1H, s, 7-OH), 8.03 (2H, d, J = 9.0 Hz, H-2′, H-6′), 7.11 (2H, d, J = 9.0 Hz, H-3′, H-5′), 6.87 (1H, s, 3H), 6.51 (1H, d, J = 2.1 Hz, 8-H), 3.86 (3H, s, 4′-OCH_3); ^{13}C NMR (100 MHz, DMSO) δ 163.2 (C, C-2), 105.28 (C, C-3), 181.95 (C, CO-4), 154.06 (C, C-5), 114.36 (C, C-6), 156.81 (C, C-7), 99.08 (C, C-8), 153.11 (C, C-9), 105.30 (C, C-10), 127.75 (C, C-1′), 130.34 (2C, C-2′,C-6′), 159.87 (C, C-4′),133.38 (2C, C-3′,C-5′), 56.22 (C, C-4′ OCH_3); HREI-MS showed $[M]^+$ peak at m/z 364 for $C_{16}H_{12}O_8S$ calculated molecular weight 364.32 g/mol.

In vitro assays

All the assays were done in triplicate, then the average value was calculated. Using a UV–VIS spectrophotometer, measurements were recorded. A methanolic stock solution of all the samples was prepared to have a concentration of 1 mg/ml. The stock solution of each sample and standard drugs were diluted to get 125, 250, and 500 µg/ml.

DPPH assay

The fractions' free radical scavenging activity was determined by DPPH assay as described before [39]. One milliliter of DPPH solution (0.135 mM) in methanol was combined with 1.0 ml of extract. For 30 min, the reaction mixture was placed in a dark place at room temperature. At 517 nm, the mixture's absorbance was determined spectrophotometrically. The ascorbic acid was used as a positive control. From the earlier studies, the following equation was used to calculate the ability to scavenging activity,

$$\text{DPPH radical scavenging activity}\,(\%) = \left[\left(\text{Abs}_{\text{Control}} - \text{Abs}_{\text{Sample}}\right)\right]/\left(\text{Abs}_{\text{Control}}\right)\left] \times 100\right.$$

In the above formula Abs Control is the absorbance of DPPH radical + methanol. Abs Sample is the absorbance of DPPH radical + sample extract/standard.

Hydroxyl radical scavenging activity

The fractions' hydroxyl radical scavenging activity was determined as described before [29]. A hydroxyl radical was created using the Fe^{3+}-Ascorbate–EDTA–H_2O_2 system (Fenton reaction) [40]. To quantify the breakdown product, the procedure uses the condensation of 2-deoxy ribose with thiobarbituric acid (TBA). The mixture of deoxydribose (0.1 ml, 2.8 mM), ethylenediaminetetraacetic acid (EDTA, 0.1 ml, 0.1 mM), hydrogen peroxide (0.1 ml, 1 mM), ascorbate (0.1 ml, 0.1 mM), potassium dihydrogen phosphate-potassium hydroxide buffer (KH_2PO_4-KOH, 0.1 ml, pH 7.4, 20 mM) were incubated for 1 h at 37 °C. TBA (1%,1 ml) and

trichloroacetic acid (2.8%,1 ml) were combined and incubated for 20 min at 100 °C. The absorbance was measured at room temperature.

Acetylcholinesterase inhibition activity

The Ellman method was used to assess AChE inhibition activity on a 96-well microplate [41]. Then, 25 µl of plant extract were mixed with 50 µl of 3 mM 5,5′-dithiobis-(2-nitrobenzoic acid) (DTNB), 50 µl of AChE (type V-S from electric eel, 1 mg/l, Sigma Aldrich), and 35 µl of 50 mM Tris-HCl (pH 8.0) comprising 0.1% bovine serum albumin and samples incubated for 5 min at 37 °C. The reaction was started by adding 25 µl of 15 mM acetylthiocholine iodide (ATCI), which resulted in the formation of a 5-thio-2-nitrobenzoate anion, which was measured at 412 nm every 5 s for 10 min using a Spectramax microplate reader (ThermoFisher). Donepezil is used as a positive control. The percentage inhibition of AChE activity was calculated using the following formula:

$$\text{Actylcholinesterase inhibition}(\%) = \left[\left(\text{Abs}_{\text{Control}} - \text{Abs}_{\text{Sample}}\right)\right]/\left(\text{Abs}_{\text{Control}}\right)] \times 100$$

5-Lipooxygenase inhibition activity

The FOX assay was carried out in a 96-well microplate to determine the 5-LOX Inhibition activity [42]. An aliquot of 50 µl LOX in 50 mM Tris-HCl buffer, pH 7.4 was pre-incubated with 20 µl plant extract and positive control ibuprofen for 5 min at 25 °C in each well of the 96-well microplate. The control wells were pipetted with 50 µl of LOX solution and 20 µl of a buffer including 0.2% v/v of DMSO. Adding the 140 µM linoleic acid in 50 mM Tris-HCl buffer (pH 7.4) initiated the enzymatic reaction and the mixtures were incubated at 25 °C for 20 min in the dark. During incubation, the LOX enzyme was present in the blanks. The substrate (linoleic acid) was added after the FOX reagent. After the color development at 25 °C, the absorbance was recorded at 595 nm. The test was stopped by adding 100 µl of freshly made FOX reagent (sulfuric acid (30 mM), xylenol orange (100 µM), iron (II) sulfate (100 µM), methanol/ water) (9:1). The Fe^{3+}–dye combination was allowed to develop for 30 min at 25 °C after termination before being measured at 560 nm.

Molecular docking studies

BIOVIA Discovery Studio 2019 was used for all molecular docking studies. The molecular docking was analyzed using the CHARMm-based forcefield of CDOCKER. The AChE three-dimensional structure being co-crystallized with galanthamine was downloaded from PDB (having the PDB code: 1QTI) [43] with the resolution 2.50 Å. Human 5-LOX complexed with arachidonic acid (PDB code: 3V99) [44] with 2.25 Å resolution was retrieved from PDB. They are classified under hydrolase and oxidoreductase. The structures were organized individually by eliminating water molecules. Hydrogen atoms were supplemented in the protein structure. Finally, at physiological pH, the protein was refined with CHARMm. The structures of the two isolated compounds were obtained from PubChem (https://pubchem.ncbi.nlm.nih.gov/). CDOCKER was used to obtain various conformations of the compounds. For each ligand, the conformations with the lowest energy were chosen as the most likely binding conformations. The co-crystallized ligands were first re-docked to the binding sites of AChE and 5-LOX respectively to confirm the docking reliability. Accordingly, the isolated compounds were docked at the same active site of AChE and 5-LOX. Both the binding mode and the interaction energy scores obtained from the docking operation were used to evaluate the affinity of our molecules to the enzymes using co-crystallized ligands and positive controls for validation of the study.

In vivo animal experiments

Based on the in vitro studies and molecular docking studies, Niruriflavone was selected for the in vivo evaluation against aluminum chloride ($AlCl_3$)-induced Alzheimer's disease model. A total of 24 healthy adult Wistar rats were used with the approval of the ethical committee of the institution and were divided into four groups each containing six animals. The animals were kept in standard isolation cages under standard environmental conditions, which included a temperature of 22 °C, relative humidity of 60%, and a 12-h light-dark cycle. Rats were given unrestricted access to water and food. Group I was considered as control that receives the only vehicle and not received $AlCl_3$. Group 2–4 animals received 100 mg/kg of oral $AlCl_3$ that was dissolved in distilled water at a dosage of 0.5 ml/100 g bw for 42 days for the induction of AD [33, 34]. Group II served as $AlCl_3$-induced AD rats without any treatment. Groups III and IV were served as treated groups that were receiving niruriflavone (0.125 mg/kg/bodyweight) and Rivastigmine (2.5 mg/kg bw) for 42nd day to 60th day by oral route, respectively [38]. After 24 h of the last dose, the rats were put through a series of behavioral tests. At the end of behavioral studies, biochemical parameters were also assessed.

Neurobehavioral assessment

Morris water maze

MWM test was used to assess the memory and cognition of rats. MWM test was conducted in a large circular pool with 210 cm diameter and 50 cm in height divided into four

quadrants, with a 1.5 cm underwater platform in the fourth quadrant. The hidden platform remained unchanged. All of the rats were given a trial a day before the actual training sessions to reduce the anxiety associated with the new environment. Each rat was gently placed in different quadrants of the swimming pool for each trial, facing the pool wall, and given 2 min to locate the hidden platform. The time (s) it took the rat to reach the platform after being submerged in water was recorded for spatial memory. The time spent (s) by the rat in the target quadrant without the platform was recorded for working (reference) memory. The time (s) took the rat to reach the platform after being submerged in water was recorded for spatial memory. The time spent (s) by the rat in the target quadrant was recorded as working memory [45, 46].

Elevated plus maze

The EPM is extensively applied to assess the anxiety-related behavior of rats. The EPM consisted of two open arms and two arms covered with walls called closed arms. The maze was elevated 50 cm above the floor. The rats were positioned on the central square platform, facing the open arm. The experiment was observed from behind the maze's screen. The maze exploration lasts for 5 min. When all four paws of a rat are on the arm, it is called an arm entry. Before testing another rat, the odor cues were removed by cleaning the maze with 20% ethanol and allowing it to dry. On the last day of drug administration, the procedure was performed. The number of entries and time spent in open and closed arms were measures of the anxiety behavior of rats [47, 48].

Biochemical assessments

Following the completion of the last behavioral task, biochemical tests were performed. Decapitation was done in the animals to remove the brain. The brain is kept in ice-cold phosphate-buffered saline and divided into two hemispheres along the medial longitudinal fissure. The homogenates were then centrifuged for 15 min at 10,000 g, and the supernatant was used. AChE, CAT, SOD (SOD), and MDA levels were assayed.

Acetylcholinesterase (AChE) activity

AChE was found to be a good indicator of cholinergic neuron loss in the brain. According to the method described by Ellman et al., 3 ml of 0.1 M sodium phosphate buffer (pH 8.0) was mixed with 0.05 ml of supernatant sample. To the mixture, 0.1 ml ATCI and 0.1 ml DTNB were added. A UV spectrophotometer was used to measure the change in absorbance at 412 nm for 2 min at 30 s intervals [49].

Catalase (CAT) activity

CAT activity was determined using Luck's method, which involves measuring the breakdown of hydrogen peroxide (H_2O_2). Then, 3 ml of H_2O_2 in phosphate buffer (pH 8.0) and 0.05 ml of supernatant were mixed. At 240 nm, the change in absorbance was measured for 2 min at 30 s intervals. Micromoles of hydrogen peroxide decomposed per min/mg of protein were used to calculate the results [50].

Superoxide dismutase (SOD) activity

One of the most important antioxidative enzymes is SOD that catalyzes the dismutation of the superoxide anion into hydrogen peroxide and molecular oxygen [51, 52]. The activity of the enzyme was measured using 0.1 mM EDTA, 50 mM sodium carbonate, and 96 mM nitro blue tetrazolium. Then, 2 ml of the above mixture, 0.05 ml of hydroxylamine, and 0.05 ml of the supernatant sample were added to the cuvette, and autooxidation of hydroxylamine was measured at 560 nm for 2 min at 30 s intervals.

Estimation of lipid peroxidation—malondialdehyde (MDA)

The amount of damage caused by ROS was the measure of MDA [53]. MDA is a major reactive aldehyde produced by biological membrane peroxidation. The TBARS assay is the most common method for determining MDA production. The supernatant was taken in a 10 ml test tube and mixed with thiobarbituric acid (TBA, 1 ml). The mixture was heated in a boiling water bath at 95 °C for 60 min. The test tubes were cooled at room temperature and absorbance was measured at 532 nm using a UV-visible spectrophotometer.

Statistical analysis

GraphPad Prism trial version 5.0 was used for statistical analysis. Data were expressed as mean ± SEM, $n = 6$, and one-way ANOVA followed by Dunnett's test. When $p < 0.05$, $p < 0.01$, and $p < 0.001$ were used, the results were considered significant.

Compliance with ethical standards

Conflict of interest The authors declare no competing interests.

References

1. Wang X, Wang W, Li L, Perry G, Lee H, Zhu X. Oxidative stress and mitochondrial dysfunction in Alzheimer's disease. Biochim Biophys Acta Mol Basis Dis. 2014;1842:1240–7.
2. Carvajal FJ, Inestrosa NC. Interactions of AChE with Aβ aggregates in Alzheimer's brain: therapeutic relevance of IDN 5706. Front Mol Neurosci. 2011;4:19 https://doi.org/10.3389/fnmol.2011.00019.
3. Garcia-Ayllon MS, Small DH, Avila J, Saez-Valero J. Revisiting the role of acetylcholinesterase in Alzheimer's disease: crosstalk with P-tau and β-amyloid. Front Mol Neurosci. 2011;4:1–9.
4. Dzoyem JP, Eloff JN. Anti-inflammatory, anticholinesterase, and antioxidant activity of leaf extracts of twelve plants used traditionally to alleviate pain and inflammation in South Africa. J Ethnopharmacol. 2015;160:194–201. https://doi.org/10.1016/j.jep.2014.11.034.
5. Joshi Y, Pratico D. Neuroinflammation and Alzheimer's disease: lessons learned from 5-lipoxygenase. Transl Neurosci. 2014;5:197–202. https://doi.org/10.2478/s13380-014-0225-7.
6. Prince M, Wimo A, Guerchet M, Ali G-C, Wu Y-T, Prina M. Alzheimer's Disease International. World Alzheimer report 2015. The global impact of dementia: an analysis of prevalence, incidence, cost and trends. https://www.alz.co.uk/research/world-report-2015.
7. Nichols E. Estimation of the global prevalence of dementia in 2019 and forecasted prevalence in 2050: an analysis for the Global Burden of Disease Study 2019. Lancet. 2022;7:E105–25.
8. Yiannopoulou KG, Papageorgiou SG. Current and future treatments in Alzheimer disease: an update. J Cent Nerv Syst Dis. 2020;12:1179573520907397.
9. Kim MJ, Rehman SU, Amin FU, Kim MO. Enhanced neuroprotection of anthocyanin-loaded PEG-gold nanoparticles against Aβ1-42-induced neuroinflammation and neurodegeneration via the NF-KB/JNK/GSK3β signaling pathway. Nanomedicine. 2017;13:2533 https://doi.org/10.1016/j.nano.2017.06.022.
10. Abdel-Aal RA, Assi AA, Kostandy BB. Rivastigmine reverses aluminum-induced behavioral changes in rats. Eur J Pharmacol. 2011;659:169–76. https://doi.org/10.1016/j.ejphar.2011.03.011. PMID: 21440537.
11. Bagalkotkar G, Sagineedu SR, Saad MS, Stanslas J. Phytochemicals from *Phyllanthus niruri* Linn. and their pharmacological properties: a review. J Pharm Pharm. 2006;58:1559–70. https://doi.org/10.1211/jpp.58.12.0001. PMID: 17331318.
12. Manjrekar AP, Jisha V, Bag PP, Adhikary B, Pai MM, Hegde A. et al. Effect of *Phyllanthus niruri* treatment on liver, kidney, and testes in CCl4 induced hepatotoxic rats. Indian J Exp Biol. 2008;46:514–20.
13. Anuar N, Markom M, Khairedin S, Johari N. A production and extraction of quercetin and (+)-catechin from *Phyllanthus niruri* callus culture. Int J Biol Biomol. 2012;6:968–71.
14. Sharma P, Parmar J, Verma P, Sharma P, Goyal PK. Anti-tumor activity of *Phyllanthus niruri* (a medicinal plant) on chemical-induced skin carcinogenesis in mice. Asian Pac J Cancer Prev. 2009;10:1089–94. PMID: 20192590.
15. Hardiyanti R, Marpaung L, Adnyana K, Simanjuntak P. Isolation of quercitrin from *Dendrophthoe pentandra (l.) miq* leaves and its antioxidant and antibacterial activities. Rasayan J Chem. 2019;12:1822–27.
16. Utari F, Itam A, Syafrizayanti S, Putri WH, Ninomiya M, Koketsu M. et al. Isolation of flavonol rhamnosides from *Pometia pinnata* leaves and investigation of α-glucosidase inhibitory activity of flavonol derivatives. J Appl Pharm Sci. 2019;9:53–65.
17. Than NN, Fotso S, Poeggeler B, Hardeland R, Laatsch H. Niruriflavone, a new antioxidant flavone sulfonic acid from *Phyllanthus niruri*. Z für Na turforschung B. 2006;61:57–60. https://doi.org/10.1515/znb-2006-0111.
18. Andrianto D, Widianti W, Bintang M. Antioxidant and cytotoxic activity of *Phyllanthus acidus* fruit extracts. IOP Conf Ser Earth Environ Sci. 2017;58:1–5. https://doi.org/10.1088/1755-1315/58/1/012022.
19. Forman HJ, Zhang H. Targeting oxidative stress in disease: promise and limitations of antioxidant therapy. Nat Rev Drug Disco. 2021;20:689–709. https://doi.org/10.1038/s41573-021-00233-1.
20. Lipinski B. Hydroxyl radical and its scavengers in health and disease. Oxid Med Cell Longev. 2011;2011:809696. https://doi.org/10.1155/2011/809696.
21. Mossa AT, Nawwar GA. Free radical scavenging and anti-acetylcholinesterase activities of *Origanum majorana* L. essential oil. Hum Exp Toxicol. 2011;30:1501–13. https://doi.org/10.1177/0960327110391686. PMID: 21239482.
22. Lin CZ, Zhu CC, Hu M, Wu AZ, Bairu ZD, Kangsa SQ. Structure-activity relationships of antioxidant activity in vitro about flavonoids isolated from *Pyrethrum tatsienense*. J Intercult Ethnopharmacol. 2014;3:123–7. https://doi.org/10.5455/jice.20140619030232.
23. Noreen H, Semmar N, Farman M, McCullagh JSO. Measurement of total phenolic content and antioxidant activity of aerial parts of medicinal plant *Coronopus didymus*. Asian Pac J Trop Med. 2017;10:792–801. https://doi.org/10.1016/j.apjtm.2017.07.024. PMID: 28942828.
24. Joshi YB, Domenico P. The 5-lipoxygenase pathway: oxidative and inflammatory contributions to the Alzheimer's disease phenotype. Front Mol Neurosci. 2015;8:436. https://doi.org/10.3389/fncel.2014.00436.
25. Gomes A, Fernandes E, Lima JL, Mira L, Corvo ML. Molecular mechanisms of anti-inflammatory activity mediated by flavonoids. Curr Med Chem. 2008;15:1586–605. https://doi.org/10.2174/092986708784911579. PMID: 18673226.
26. Alhawarri MB, Dianita R, Razak KNA, Mohamad S, Nogawa T, Wahab HA. Antioxidant, anti-inflammatory, and inhibition of acetylcholinesterase potentials of *Cassia timoriensis* DC. flowers. Molecules. 2021;26:2594 https://doi.org/10.3390/molecules26092594. PMID: 33946788; PMCID: PMC8125573.
27. Nam G, Hong M, Lee J, Lee HJ, Ji Y, Kang J. et al. Multiple reactivities of flavonoids towards pathological elements in Alzheimer's disease: structure–activity relationship. Chem Sci. 2020;37:10243–54.
28. Cavallaro V, Braun AE, Ravelo AG, Murray AP. Sulphated flavonoid isolated from *Flaveria bidentis* and its semisynthetic derivatives as potential drugs for Alzheimer's disease. In Proceedings of the 17th International Electronic Conference on Synthetic Organic Chemistry. Basel, Switzerland: MDPI; 2013. https://doi.org/10.3390/ecsoc-17-b011.
29. Figueira I, Garcia G, Pimpão RC, Terrasso AP, Costa I, Almeida AF. et al. Polyphenols journey through blood-brain barrier towards neuronal protection. Sci Rep. 2017;7:11456. https://doi.org/10.1038/s41598-017-11512-6.
30. Shailima R, Mary RL. Network based approach in the establishment of the relationship between type 2 diabetes mellitus and its complications at the molecular level coupled with molecular docking mechanism. Biomed Res Int. 2016;2016:6068437. https://doi.org/10.1155/2016/6068437.
31. Bhuvanendran S, Hanapi NA, Ahemad N, Othman I, Yusof SR, Shaikh MF. Embelin, a potent molecule for Alzheimer's disease: a proof of concept from blood-brain barrier permeability, acetylcholinesterase inhibition and molecular docking studies. Front Neurosci. 2019;13:495 https://doi.org/10.3389/fnins.2019.00495.
32. Singh NA, Bhardwaj V, Ravi C, Ramesh N, Mandal AKA, Khan ZA. EGCG nanoparticles attenuate aluminum chloride induced neurobehavioral deficits, beta amyloid and tau pathology in a rat

model of Alzheimer's disease. Front Aging Neurosci. 2018;10:244. https://doi.org/10.3389/fnagi.2018.00244.
33. Thippeswamy AH, Rafiq M, Viswantha GL, Kavya KJ, Anturlikar SD, Patki PS. Evaluation of *Bacopa monniera* for its synergistic activity with rivastigmine in reversing aluminum-induced memory loss and learning deficit in rats. J Acupunct Meridian Stud. 2013;6:208–13. https://doi.org/10.1016/j.jams.2013.02.004. PMID: 23972243.
34. Kumar A, Prakash A, Dogra S. Neuroprotective effect of carvedilol against aluminium induced toxicity: possible behavioral and biochemical alterations in rats. Pharm Rep. 2011;63:915–23. https://doi.org/10.1016/s1734-1140(11)70607-7. PMID: 22001979.
35. Kakkar V, Kaur IP. Evaluating potential of curcumin loaded solid lipid nanoparticles in aluminium induced behavioural, biochemical and histopathological alterations in mice brain. Food Chem Toxicol. 2011;49:2906–13. https://doi.org/10.1016/j.fct.2011.08.006. PMID: 21889563.
36. Kaizer RR, Corrêa MC, Spanevello RM, Morsch VM, Mazzanti CM, Gonçalves JF. et al. Acetylcholinesterase activation and enhanced lipid peroxidation after long-term exposure to low levels of aluminum on different mouse brain regions. J Inorg Biochem. 2005;99:1865–70. https://doi.org/10.1016/j.jinorgbio.2005.06.015. 16055195.
37. Kaur A, Gill KD. Possible peripheral markers for chronic aluminium toxicity in Wistar rats. Toxicol Ind Health. 2006;22:39–46. https://doi.org/10.1191/0748233706th242oa. PMID: 16572710.
38. Chen X, Zhang M, Ahmed M, Surapaneni KM, Veeraraghavan VP, Arulselvan P. Neuroprotective effects of ononin against the aluminium chloride-induced Alzheimer's disease in rats. Saudi J Biol Sci. 2021;28:4232–9. https://doi.org/10.1016/j.sjbs.2021.06.031.
39. Al-Mamary M, Al-Habori M, Al-Zubairi AS. The in vitro antioxidant activity of different types of palm dates (*Phoenix dactylifera*) syrups. Arab J Chem. 2014;7:964–71.
40. Hazra B, Biswas S, Mandal N. Antioxidant and free radical scavenging activity of *Spondias pinnata*. BMC Complement Alter Med. 2008;8:63 https://doi.org/10.1186/1472-6882-8-63.
41. Mathew M, Subramanian S. In vitro screening for anti-cholinesterase and antioxidant activity of methanolic extracts of ayurvedic medicinal plants used for cognitive disorders. PLoS One. 2014;9:e86804 https://doi.org/10.1371/journal.pone.0086804.
42. Chung LY, Soo WK, Chan KY, Mustafa MR, Goh SH, Imiyabir Z. Lipoxygenase inhibiting activity of some Malaysian plants. Pharm Biol. 2009;47:1142–48. https://doi.org/10.3109/13880200903008724.
43. Ishola AA, Oyinloye BE, Basiru A, Kappo AP. Molecular docking studies of flavonoids from *Andrographis paniculata* as potential acetylcholinesterase, butyrylcholinesterase and monoamine oxidase inhibitors towards the treatment of neurodegenerative diseases. Biointerface Res Appl Chem. 2020;11:9871–9. https://doi.org/10.33263/BRIAC113.98719879.
44. Yadavalli R, Peasari JR, Mamindla P, Praveenkumar, Mounika S, Ganugapati J. Phytochemical screening and in silico studies of flavonoids from *Chlorella pyrenoidosa*. Inf Med Unlocked. 2018;10:89–99.
45. Morris R. Developments of a water-maze procedure for studying spatial learning in the rat. J Neurosci Methods. 1984;11:47–60.
46. Bhalla P, Garg ML, Dhawan DK. Protective role of lithium during aluminium-induced neurotoxicity. Neurochem Int. 2010;56:256–62. https://doi.org/10.1016/j.neuint.2009.10.009.
47. Prakash A, Kumar A. Effect of N-acetyl cysteine against aluminium-induced cognitive dysfunction and oxidative damage in rats. Basic Clin Pharm Toxicol. 2009;105:98e104.
48. Cheng L, Pan GF, Sun XB, Huang YX, Peng YS, Zhou LY. Evaluation of anxiolytic-like effect of aqueous extract of asparagus stem in mice. Evid Based Complement Altern Med. 2013;2013:587260 https://doi.org/10.1155/2013/587260. PMID: 24348707; PMCID: PMC3853311.
49. Ellman GL, Courtney KD, Andres V Jr, feather-Stone RM. A new and rapid colorimetric determination of acetylcholinesterase activity. Biochem Pharm. 1961;7:88–95. https://doi.org/10.1016/0006-2952(61)90145-9. PMID: 13726518.
50. Luck H. Catalase. In: Bergmeyer HU, editor. Methods of enzymatic analysis. New York: Academic Press; 1971. p. 885–93.
51. Ellman GL. Tissue sulfhydryl groups. Arch Biochem Biophys. 1959;82:48670–7.
52. Kono Y. Generation of superoxide radical during auto-oxidation of hydroxylamine and an assay for superoxide dismutase. Arch Biochem Biophys. 1978;186:189–95.
53. Wills ED. Mechanism of lipid peroxide formation in animal tissues. Biochem J. 1966;99:667–76.